SMALL-SIGNAL STABILITY MODELING OF THE MICROGRID WITH NETWORK TRANSIENTS TAKEN INTO CONSIDERATION

Hung Nguyen-Van[1,2*], Huy Nguyen-Duc[1]

[1]*Hanoi University of Sience and Technology*
[2]*Hanoi University of Industry*

*Corresponding author: vanhung312@gmail.com

(Received: December 23, 2020; Accepted: April 23, 2021)

Abstract - The development of a small signal model that accurately reflects dynamic processes plays an essential role in the stability analysis and control of power systems. The main components in a microgrid power system are synchronous generators, the electrical network, electrical loads, and inverters. A method to derive the microgrid state-space model is proposed in the article. This method is based on linearized models of synchronous generators, electronic power inverters, networks, and loads. This model can be further developed to account for microgrid control schemes such as frequency control and voltage regulation. A small-signal analysis of the Microgrid model is also carried out in this work.

Key words - Microgrid; state-space model; DG; inverter; eigenvalue analysis

1. Introduction

The increasing penetration of distributed energy resources such as wind and solar is a trend that has been observed in many electric power systems [1]. However, the control and operation of distributed generation sources (DG), especially those of inverter-based generators, have many differences compared to the operation and control of conventional power systems. A microgrid (MG) can be established by connecting DG and local loads, which operate both in grid-connected and islanded modes. This can help increase the flexibility in the operation of DG and the reliability of the whole system [2], [3]. The typical structure of a MG is shown in Figure 1.

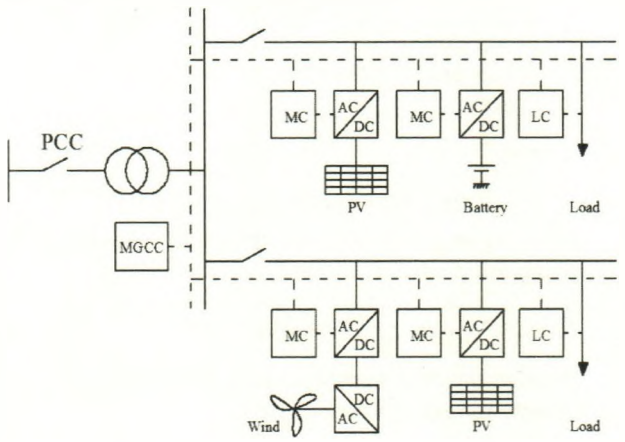

Figure 1. *Typical structure of microgrid*

Some of the distinctive features of the MG operation and control can be described as follows: *i)* The rotating inertia of the MG system is usually small, compared to that of a large synchronously connected grid, because the inverter-based sources have inherently zero inertia; *ii)* The MG usually consists of low/medium voltage networks which have low X/R ratios. On the other hand, conventional transmission systems have high X/R ratios, which makes the active power transfer primarily dependent on angle difference; *iii)* The primary generation sources in microgrid are variable sources (e.g., wind and solar) which are stochastic and uncertain. The uncertain nature of these sources has a significant impact on the control and operation of MGs [4], [5].

In the grid-connected mode, the voltage and the frequency stability depend on the dynamics of the grid. On the other hand, in the islanded mode, the voltage and the frequency stability are heavily influenced by the internal dynamics of MG [6]. The control of the power distribution between DG and of bus voltages is carried out by the control system of DG [7]. Depending on the specific control scheme [7], a DG can operate like a current source inverter (CSI) or a voltage source inverter (VSI). In the islanded mode, the VSI/CSI control scheme plays a vital role in small signal stability.

In the small signal stability analysis of traditional electric systems, the time constants of electromechanical oscillation are much higher than time constants of network transients. Therefore, the network transients can be omitted [8]. Because of the reduced inertia in MG, ignoring network transients is no longer suitable. Some MG small-signal models are proposed in [9], [10]. In [9], the MG small-signal model with the central element being VSI is proposed. However, this model does not account for DGs, which are based on synchronous generators. The proposed model in [10] is based on synchronizing individual models in rotating reference frame *dq*. The connection of each individual model is based on an equation of bus voltage vectors at the nodes in the grid, so it is difficult when the number of nodes in the grid is high.

This article proposes a method to formulate a MG state-space model, with the following features:

- Including a variety of DGs, which are synchronous generators, voltage source inverters;
- Considering the network transients, including transmission lines and RLC loads;
- DG models are modified so that the input and output vectors match the input and output vectors of the grid;
- The models are synchronized following only one rotating reference frame.

2. The state space model of microgrid

For the sake of convenience in developing the state-space models of different elements, the *dq* rotating reference frame is employed. First, each element is modeled in a separate local rotating reference frame (dq^n). The exchange of the quantities on the *abc* axes to rotating reference frame *dq* is based on the Park transformation formula [8].

When combining the elements, it is necessary to transfer the local rotating reference frames dq^n into the global rotating reference frames dq^g [11]. The relationship between the frames is:

$$\begin{bmatrix} f_d^g \\ f_q^g \end{bmatrix} = \begin{bmatrix} \cos\delta_n & -\sin\delta_n \\ \sin\delta_n & \cos\delta_n \end{bmatrix} \begin{bmatrix} f_d^n \\ f_q^n \end{bmatrix} \quad (1)$$

Linearizing (1) leads to:

$$\begin{bmatrix} \Delta f_d^g \\ \Delta f_q^g \end{bmatrix} = \begin{bmatrix} \cos\delta_n^0 & -\sin\delta_n^0 \\ \sin\delta_n^0 & \cos\delta_n^0 \end{bmatrix} \begin{bmatrix} \Delta f_d^n \\ \Delta f_q^n \end{bmatrix} + \begin{bmatrix} -f_{q0}^g \\ f_{d0}^g \end{bmatrix} \Delta\delta_n \quad (2)$$

where: $f^n = \left[f_d^n f_q^n \right]^T : f^g = \left[f_d^g f_q^g \right]^T$ are respectively the quantities in the local rotating reference frame (dq^n) and the global rotating reference frames (dq^g); δ_n is the angle difference between two axes dq^n and dq^g. The subindex "*0*" denotes steady-state operating values.

2.1. Synchronous generator model

The small-signal model of a two-pole, three-phase synchronous machine is presented in [12]. The differential equations that describe the voltage equations between the elements in a synchronous generator and are introduced in the matrix form:

$$V^s = G.I^s + H\frac{d}{dt}(I^s) \quad (3)$$

Where: $V^s = \left[v_q v_d v_{kq1} v_{kq2} v_{fd} v_{kd} \right]^T$; $I^s = \left[i_q i_d i_{kq1} i_{kq2} i_{fd} i_{kd} \right]^T$ are vectors of voltages and currents of the stator windings (*q.d*), damper windings (*kq1, kq2, kd*) and field winding (*fd*).

The swing equations:

$$\frac{2H}{\omega_B}\frac{d\omega}{dt} = \overline{T}_m - \overline{T}_e \quad (4)$$

$$\frac{d\delta}{dt} = \omega_B \frac{(\omega_r - \omega_B)}{\omega_B} \quad (5)$$

where ω is rotor angular speed; H is the inertia constant of rotor and load; $\overline{T}_m$, $\overline{T}_e$ are the mechanical and airgap torques:

$$T_e = X_{md}(-i_d + i_{fd} + i_{kd}) - X_{mq}(-i_q + i_{kq1} + i_{kq2}) \quad (6)$$

Linearizing the above ddifferential equations yields:

$$E\Delta\dot{x}_g = F\Delta x_g + u \quad (7)$$

The vector of the states variables is as follows:

$$\Delta x_g = \left[\Delta i_q \Delta i_d \Delta i_{kq1} \Delta i_{kq2} \Delta i_{fd} \Delta i_{kd} \frac{\Delta\omega_r}{\omega_B} \Delta\delta \right]^T$$

The vector of input parameters is:

$$u = \left[\Delta v_q \Delta v_d \Delta v_{kq1} \Delta v_{kq2} \Delta v_{fd} \Delta v_{kd} \Delta T_m \right]^T$$

Combining (2), (3), and (7) and transposing the matrix, we get the state-space model:

$$\Delta\dot{x}_g = A_s \Delta x_g + B_s^v \Delta v^s + B_s^u \Delta u^s \quad (8)$$

In formula (8), the input variables can be broken down into:

$$\Delta v^s = \left[\Delta v_q \ \Delta v_d \right]^T : \Delta u^s = \left[\Delta v_{fd} \ \Delta T_m \right]^T$$

Thus, the synchronous generator model has the vector of input variables being voltages, and the vector of output variables being the electric currents.

2.2. VSI inverter model

The overall control diagram of a grid-connected DG through the VSI is shown in Figure 2 [10]. The VSI model consists of two main elements: i) the power circuit connecting VSI and the grid; ii) the VSI controlling system.

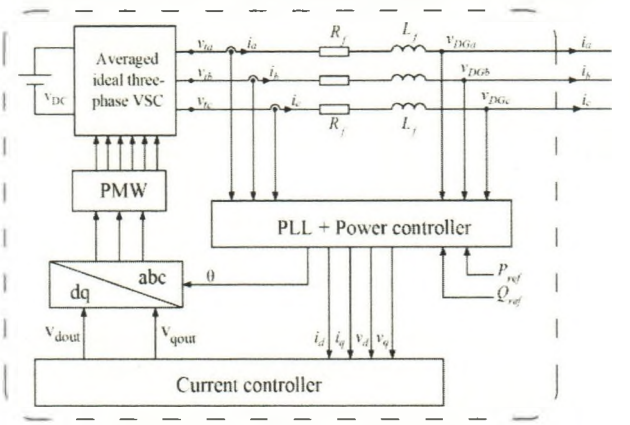

Figure 2. *The overall control diagram of VSI*

The main control system consists of two inner current control loops following the two axes of *dq*, and two outer power control loops, which send the reference value to the two inner current control loops. The secondary control loops determine the set point values (active and reactive power).

2.2.1. The VSI coupling circuit

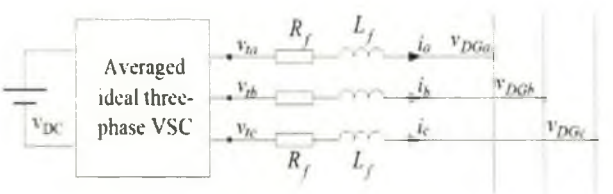

Figure 3. *The circuit diagram of VSI*

The coupling circuit is described by means of the following differential equations:

$$R_f i_{abc} + L_f \frac{d}{dt} i_{abc} = v_{t,abc} - v_{IGi,abc} \quad (9)$$

Through the Park transformation, (9) is converted into the rotating reference frames dq^n:

$$\begin{aligned} \frac{d}{dt} i_d &= -\frac{R_f}{L_f} i_d + \omega_r i_q + \frac{1}{L_f}\left(v_{t,d} - v_{IGi,d} \right) \\ \frac{d}{dt} i_q &= -\frac{R_f}{L_f} i_q - \omega_r i_d + \frac{1}{L_f}\left(v_{t,q} - v_{IGi,q} \right) \end{aligned} \quad (10)$$

By changing variables to decouple the quantities on two dq axes, we can obtain:

$$v_{td} = v_{t,d} - v_{IXi,d} + \omega_r L_f i_q$$
$$v_q = v_{t,q} - v_{IXi,q} - \omega_r L_f i_d \quad (11)$$

Combining (10) (11) and re-writing in the matrix form:

$$\frac{d}{dt}\begin{bmatrix} i_d \\ i_q \end{bmatrix} = \begin{bmatrix} -R_f / L_f & 0 \\ 0 & -R_f / L_f \end{bmatrix}\begin{bmatrix} i_d \\ i_q \end{bmatrix} + \begin{bmatrix} 1/L_f & 0 \\ 0 & 1/L_f \end{bmatrix}\begin{bmatrix} v_d \\ v_q \end{bmatrix} \quad (12)$$

Linearizing (12), combining with (2), and changing the frames of dq^n into dq^g, one obtains:

$$\Delta \dot{x}_{IXi} = A_I \Delta x_{IXi} + B_I^{vIXi} \Delta v_{IXi} + B_I^{\theta} \Delta\theta + B_I^{\omega r} \Delta\omega_r + B_I^{vdq} \Delta v_{dq} \quad (13)$$

With: $\Delta x_{IXi} = \left[\Delta i_d \Delta i_q\right]^T ; \Delta v_{dq} = \left[\Delta v_d \Delta v_q\right]^T$

$\Delta v_{IXi} = \left[\Delta v_{IXi,d} \Delta v_{IXi,q}\right]^T :$

The power circuit model is shown in Figure 4.

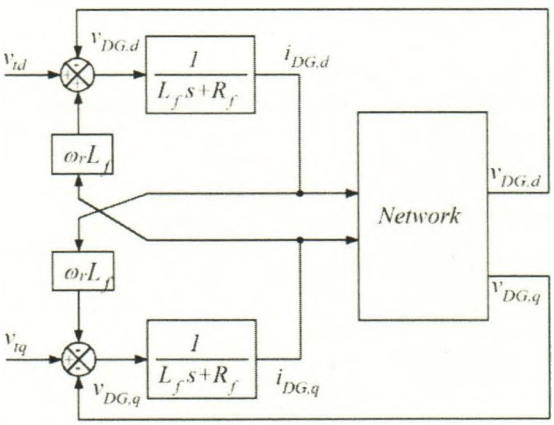

Figure 4. *The VSI power circuit model*

2.2.2. The VSI controlling system model

a. Phase-locked loop (PLL)

The determination of the rotational frequency of the local rotating reference frames dq^n and the phase difference angle θ^n plays an important role in connecting VSIs to the electricity grid, and this process is done by the PLL [13].

The linearized dynamic model of PLL:

$$\Delta\dot{\omega}_r = k_{pll}.k_{pw}\Delta\omega_{ref} - k_{pll}.k_{pw}\Delta\omega_r + k_{pll}.k_{iw}\left(\Delta\theta_{ref} - \Delta\theta\right) \quad (14)$$

$$\Delta\dot{\theta} = \Delta\omega_r$$

b. Power controller

A power controller consists of two loops, which are responsible for controlling the active power P, and the reactive power Q, as shown in Figure 5. P_{ref}, Q_{ref} are the respective reference values provided by the secondary control [5]. P_{out}, Q_{out} are determined by the electric currents and voltages in the dq frame, as follows:

$$Q_{out} = \frac{3}{2}\left(v_{IXi,q} i_d - v_{IXi,d} i_q\right)$$
$$P_{out} = \frac{3}{2}\left(v_{IXi,d} i_d + v_{IXi,q} i_q\right) \quad (15)$$

The dynamic model of the power controller is:

$$\frac{d}{dt} i_{iq} = Q_{ref} - Q_{out}$$
$$\frac{d}{dt} i_{id} = P_{ref} - P_{out} \quad (16)$$

Combining (15)-(16) and linearizing, we have:

$$\Delta\dot{i}_{iq} = \Delta Q_{ref} - \frac{3}{2}(v^0_{IXi,q}\Delta i_d + i^0_d \Delta v_{IXi,q} - v^0_{IXi,d}\Delta i_q - i^0_q \Delta v_{IXi,d})$$
$$\Delta\dot{i}_{id} = \Delta P_{ref} - \frac{3}{2}(v^0_{IXi,d}\Delta i_d + i^0_d \Delta v_{IXi,d} + v^0_{IXi,q}\Delta i_q + i^0_q \Delta v_{IXi,q}) \quad (17)$$

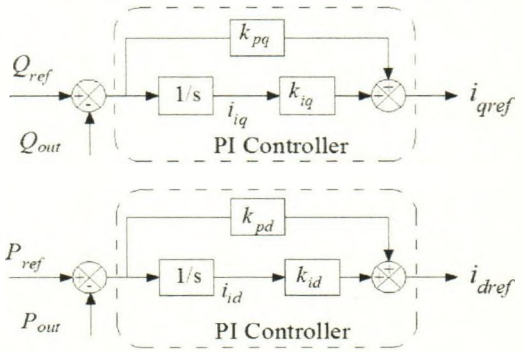

Figure 5. *The power controller*

From that, it is possible to identify Δi_{qref}, Δi_{dref}

$$\Delta i_{qref} = -\frac{3}{2}k_{pq}(v^0_{DG,q}\Delta i_d + i^0_d \Delta v_{IXi,q} - v^0_{DG,d}\Delta i_q - i^0_q \Delta v_{IXi,d}) + k_{pq}\Delta Q_{ref} + k_{iq} i_{iq}$$
$$\Delta i_{dref} = -\frac{3}{2}k_{pd}(v^0_{DG,d}\Delta i_d + i^0_d \Delta v_{IXi,d} + v^0_{IXi,q}\Delta i_q + i^0_q \Delta v_{IXi,q}) + k_{pd}\Delta P_{ref} + k_{id} i_{id} \quad (18)$$

c. Current controller

The low-pass filter in the current controller consists of two PI compensators shown in Figure 6 [14], [15]. The symbol *"f"* denotes the filtered quantities.

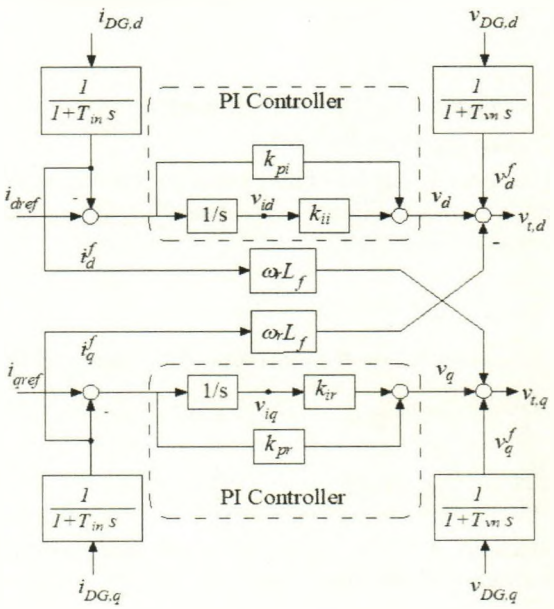

Figure 6. *Current controller*

The differential equations of the linearized current controller are:

$$\frac{d}{dt}\Delta v_{id} = \Delta i_{dref} - \Delta i_d^f$$
$$\frac{d}{dt}\Delta v_{iq} = \Delta i_{qref} - \Delta i_q^f \quad (19)$$

The vectors of voltages at the connection point of a DG $[v_{t,d}\ v_{t,q}]$ can be represented by the following state variables:

$$\Delta v_{t,d} = \Delta v_d^f - \omega_r L_f \Delta i_q^f + k_{ii}\Delta v_{i,d} + k_{pi}\Delta \dot{v}_{i,d}$$
$$\Delta v_{t,q} = \Delta v_q^f + \omega_r L_f \Delta i_d^f + k_{ir}\Delta v_{i,q} + k_{pr}\Delta \dot{v}_{i,q} \quad (20)$$

From (14), (17), (19), (20), one can obtain a controller state-space model:

$$\Delta \dot{x}_c = A_c\Delta x_c + B_c^{xIX_i}\Delta x_{IX_i} + B_c^{vIX_i}\Delta v_{IX_i} + B_c^{vdq}\Delta v_t + B_c^{uIX_i}\Delta u_{IX_i} + B_c^{\theta}\Delta\theta \quad (21)$$

where: $\Delta x_c = \left[\Delta v_d^f \Delta v_q^f \Delta i_d^f \Delta i_q^f \Delta v_{id}\Delta v_{iq}\Delta i_{id}\Delta i_{iq}\Delta\omega_r\Delta\theta\right]^T$

$$\Delta u_{IX_i} = \left[\Delta P_{ref}\Delta Q_{ref}\Delta\theta_{ref}\Delta\omega_{ref}\right]^T$$

The full mathematical model of DG is represented in the system of equations (13), (21). In this model, the current vector is the input, and the voltage vector is the output.

2.3. The network model

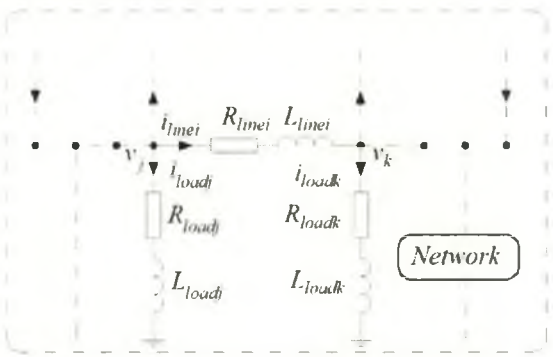

Figure 7. *General inductive branch diagram*

2.3.1. Inductive branch model

The general diagram of the branch connecting node *j* to node *k* is shown in Figure 7. The branch equations can be written as follows:

$$L_i\frac{di_{i,abc}}{dt} + R_i i_{i,abc} = v_{j,abc} - v_{k,abc} \quad (22)$$

Converting (22) to the *dq* coordinate system yields:

$$\frac{di_{id}}{dt} = -\frac{R_i}{L_i}i_{id} + \omega_s i_{iq} + \frac{1}{L_i}v_{j,d} - \frac{1}{L_i}v_{k,d}$$
$$\frac{di_{iq}}{dt} = -\frac{R_i}{L_i}i_{iq} - \omega_s i_{id} + \frac{1}{L_i}v_{j,q} - \frac{1}{L_i}v_{k,q} \quad (23)$$

Extending (23) for *n* branches in the grid, linearizing and writing in matrix form yield:

$$\Delta \dot{x}_{Br} = A_{Br}\Delta x_{Br} + B_{Br}\Delta v_N \quad (24)$$

$$\Delta x_N = \left[\Delta i_{1dq}\Delta i_{2dq}...\Delta i_{ndq}\right]^T;\ \Delta v_N = \left[\Delta v_{1dq}\Delta v_{2dq}...\Delta v_{ndq}\right]^T$$

$$A_{Br} = diag\left[A_{Br1}A_{Br2}...A_{Brn}\right]_{2n\times 2n};\ B_{Br} = \left[B_{Br1}B_{Br2}...B_{Brn}\right]^T$$

$$A_{Bri} = \begin{bmatrix} -\frac{R_i}{L_i} & \omega_s \\ -\omega_s & -\frac{R_i}{L_i} \end{bmatrix};\ B_{Bri} = \begin{bmatrix} \cdots & \frac{1}{L_i} & 0 & \cdots & -\frac{1}{L_i} & 0 & \cdots \\ \cdots & 0 & \frac{1}{L_i} & \cdots & 0 & -\frac{1}{L_i} & \cdots \end{bmatrix}_{2\times(2m)}$$

2.3.2. Load model

In this work, we consider the RL load. The differential equation for this type of load is as follows:

$$L_j\frac{di_{loadj}}{dt} + R_j i_{loadj} = v_{j,abc} \quad (25)$$

Writing (25) for *m* loads connecting to *m* nodes and linearizing, one obtains the following:

$$\frac{di_{loadjd}}{dt} = -\frac{R_j}{L_j}i_{loadjd} + \omega_s i_{loadjq} + \frac{1}{L_j}v_{j,d}$$
$$\frac{di_{loadjq}}{dt} = -\frac{R_j}{L_j}i_{loadjq} - \omega_s i_{loadjd} + \frac{1}{L_j}v_{j,q} \quad (26)$$

Writing (23) for *n* branches in the grid, linearizing, and writing in matrix form yield the following equation:

$$\Delta \dot{x}_{Load} = A_{Load}\Delta x_{Load} + B_{Load}\Delta v_N \quad (27)$$

Where: $\Delta x_{load} = \left[\Delta i_{load1dq}\Delta i_{load2dq}...\Delta i_{loadmdq}\right]^T$

$$A_{load} = diag\left[A_{load1}A_{load2}...A_{loadm}\right]_{2m\times 2m}$$

$$B_{load} = \left[B_{load1}B_{load2}...B_{loadm}\right]^T$$

$$A_{loadj} = \begin{bmatrix} -\frac{R_j}{L_j} & \omega_b \\ -\omega_b & -\frac{R_j}{L_j} \end{bmatrix};\ B_{loadj} = \begin{bmatrix} \cdots & \frac{1}{L_j} & 0 & \cdots \\ \cdots & 0 & \frac{1}{L_j} & \cdots \end{bmatrix}_{2\times 2m}$$

Combining (24) and (27) lead to the grid state-space model:

$$\Delta \dot{x}_N = A_{NET}\Delta x_N + B_{NET}\Delta v_N \quad (28)$$

where: $\Delta x_N = \left[\Delta x_{Br}\Delta x_{load}\right]^T$

$$A_{NET} = diag\left[A_{Br}A_{load}\right];\ B_{NET} = \left[B_{Br}B_{load}\right]^T;$$

The vector of the state variables includes the current across the inductive components, the voltage across the capacitive components with inductive networks $v_N=[v_d,v_q]^T$; $y_N=[i_d,i_q]^T$. The voltage vector is the input variable, and the current vector is the output variable.

2.4. Microgrid general model

The diagram describing elements interconnection is shown in Figure 8. All elements need to have currents as input and voltages as output to interface with the grid model [16]. Therefore, it is necessary to modify the source model of the DG by adding a parallel connection with a capacitor of sufficiently small value. With the DG model being modified to take currents as input, the small-signal model of MG is shown in Figure 8.

The MG model shown in Figure 8 is the result of the combination of (8), (13), (21), (28):

$$\begin{aligned}\Delta \dot{x}_{MG} &= A_{MG}\Delta x_{MG} + B_{MG}\Delta u_{MG} \\ \Delta y_{MG} &= C_{MG}\Delta x_{MG} + D_{MG}\Delta u_{MG}\end{aligned} \quad (29)$$

where: $\Delta x_{MG} = \left[\Delta x_g \Delta x_{DG} \Delta x_c \Delta x_{Net}\right]^T$

$\Delta u_{MG} = \left[\Delta u^s \Delta u^{DG}\right]^T$

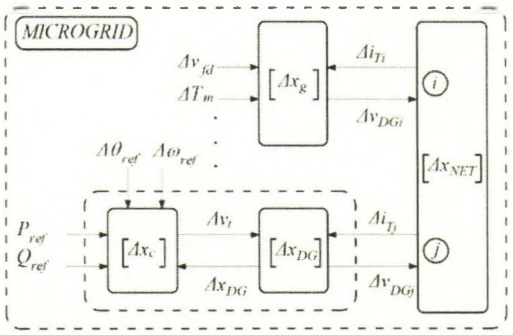

Figure 8. *Microgrid general model*

3. Case study

3.1. System parameters

The proposed state modeling method is applied to a three-node MG, shown in Figure 9. Parameters of the elements in the schematic are given in Table 1, 2. The proposed modeling approach is implemented in Matlab/ Simulink.

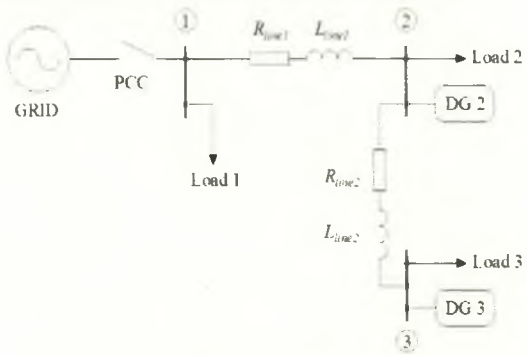

Figure 9. *Microgrid in case study*

Table 1. *Branch and load parameters*

S_b = 10 MVA: V_b= 13.8 kV		Load 1	1.65 + j 2.02 MVA
Line 1	0.2087 + j 0.3692 pu	Load 2	2.3 + j 1.47 MVA
Line 2	0.3468 + j0.5329 pu	Load 3	1.8 + j 0.6 MVA

Table 2. *Source parameters*

DG2 – Synchronous Gen S_b = 5 MVA; V_b= 13.8 kV		**DG3, S_n = 3 MVA Power electronic interface**	
r_a	0.0052 pu	L_f	0.1 mH
X_d	2.86 pu	R_f	2.4 mΩ
X_q	2.0 pu	k_{pll}	1
X_{lkd}	0.0208 pu	k_{pw}	313
X_{lfd}	0.6157 pu	k_{iw}	10000
X_{kd}	2.68 pu	k_{pd}	0.06
X_{fd}	3.2757 pu	k_{pq}	0.028
X_{ls}	0.2 pu	k_{pi}	0.205
r_{kd}	0.1381 pu	k_{ii}	1.6
r_{fd}	0.0026 pu	k_{pr}	0.205
H	2.9 pu	k_{ir}	1.6

3.2. Eigenvalue analysis

Table 3 shows the eigenvalues of the MG model in Figure 9 in the grid-connected mode. All 28 eigenvalues have negative real parts. Eigenvalues from 1 to 18 are 9 pairs of complex conjugates, representing 9 modes of oscillation in the system.

The eigenvalues 1 to 14 characterize the electrical oscillation between the DGs and the grid. The eigenvalues 15 to 18 characterize the mechanical oscillation between the DG2 rotor and the system.

Table 3. *Eigenvalues of MG*

Eigen values	Real (1/s)	Im (rad/s)	Eigen values	Real (1/s)	Im (rad/s)
1.2	-91.13	± 5628.5	19.20	-333.33	0
3.4	-97.84	± 4870.9	21	-276.88	0
5.6	-158.29	± 3653.6	22	-257.73	0
7.8	-145.69	± 3709.7	23	-92.65	0
9.10	-222.40	± 377.0	24	-36.12	0
11.12	-6.01	± 375.7	25	-8.26	0
13.14	-71.24	± 363.8	26	-8.26	0
15.16	-0.80	± 13.7	27	-1.15	0
17.18	-55.15	± 1.6	28	-0.42	0

3.3. Sensitivity analysis

To determine the optimal control parameters in the grid separated mode, we examine the parameters in the PI controller within the power control, which are k_{pd} and k_{pq}.

Figure 10a shows the trajectories of the eigenvalue pair (7,8) when k_{pd} varies from 0.01 to 0.9. Notice that when the k_{pd} value increases, the eigenvalue pair tends to move towards the increasing damping coefficient and vice versa.

Similarly, Figure 10b shows the trajectories of the eigenvalue pair (5,6) when k_{pq} varies from -0.9 to -0.01. It can be observed that when the k_{pq} is increased, the eigenvalue pair tends to move towards the decreasing damping coefficient and vice versa.

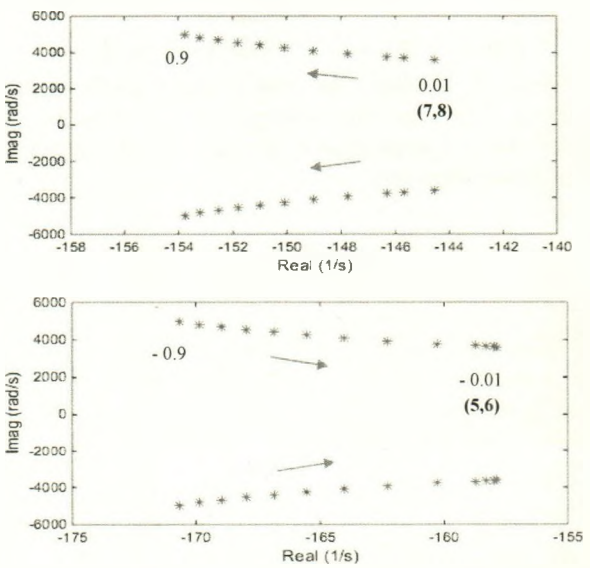

Figure 10. *The orbits of the eigenvalue pair (7,8) and (5,6) when k_{pd} and k_{pq} change*

3.4. Step response and frequency response

The small-signal model in (29) is used to analyze responses in the time domain and frequency domain. We apply a step change in power (P_{ref3}) and observe the changes in voltage variables (P_{ref3}).

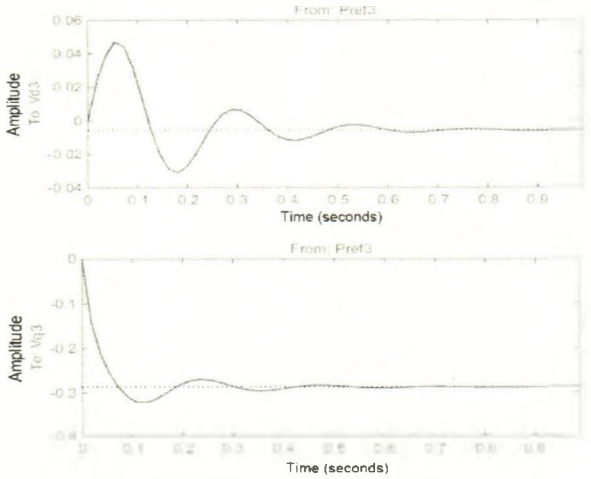

Figure 11. *Response voltage V_{dq3} from P_{ref3}*

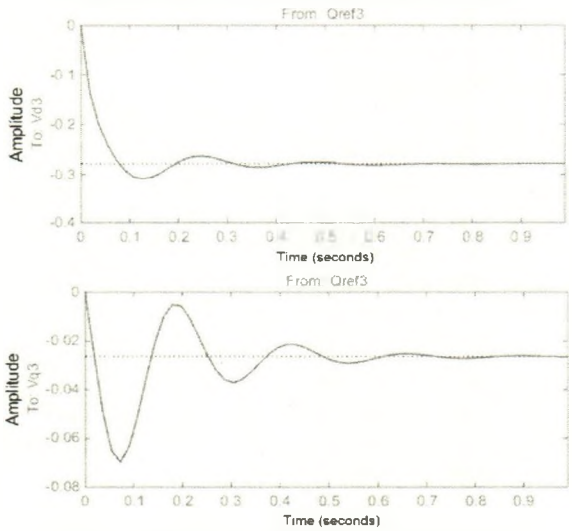

Figure 12. *Response of voltage V_{dq3} from Q_{ref3}*

Figure 11, 12 shows the time response of the voltage parameter V_{dq3} when step changes of P_{ref3} and Q_{ref3} are applied. The response time and output voltage responses can be easily observed.

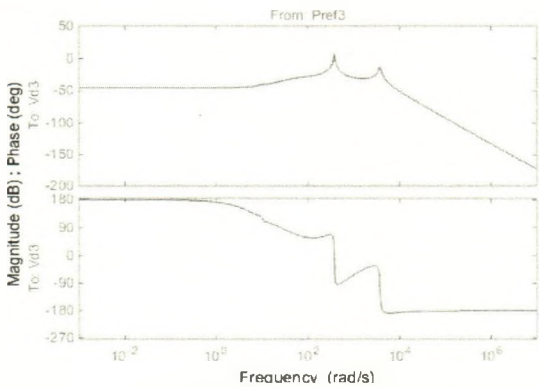

Figure 13. *V_{dq3} / P_{ref3} bode diagram*

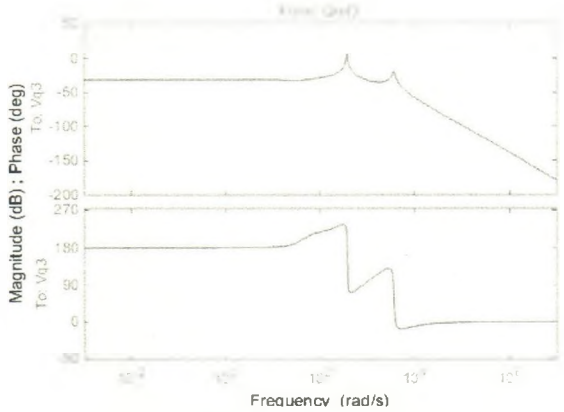

Figure 14. *V_{dq3} / Q_{ref3} bode diagram*

Figure 13, 14 shows the bode diagrams of transfer functions between V_{dq3} / P_{ref3}, and between V_{dq3} / Q_{ref3}. The Bode plot shows that the bandwidth of input/output is approximately 100Hz. This information can be utilized to provide a balanced solution between the bandwidth of input/output transfer functions while maintaining the small-signal tability of the system.

4. Conclusion

The development of a small signal model of microgrids plays a vital role in their stability analysis and in determining their optimal control parameters. The MGs have many different characteristics from the traditional grid in terms of small-signal stability. The fundamental difference comes from DGs dynamics being influenced by the electronic-based power converters with zero inertia. Besides, in studying MG stability, it is necessary to consider the electromagnetic transients on the RLC circuits of the transmission lines.

The article proposes a method to derive a small-signal model of DGs consisting of synchronous generators, inverters and RLC network circuits. The article also proposes an approach to connect different element models, thereby building a full microgrid model including typical components of DG, taking into account the network transients. The eigenvalue, sensitivities, time, and frequency responses of the built model have been analyzed.

In future works, the proposed small-signal model can be augmented with the secondary control loop to study different MG control strategies and their robust stability characteristics.

REFERENCES

[1] S. Chowdhury, S. P. Chowdhury, and P. Crossley, *Microgrids and Active Distribution Networks*. 2009.

[2] R. H. Lasseter, "MicroGrids", *2002 IEEE Power Eng. Soc. Winter Meet. Conf. Proc. (Cat. No.02CH37309)*, vol. 1, pp. 305–308, 2002.

[3] P. Piagi and R. H. Lasseter, "Autonomous control of microgrids", *2006 IEEE Power Eng. Soc. Gen. Meet.*, p. 8 pp., 2006

[4] T. L. Vandoorn and J. C. Vásquez, "Hierarchical Control and an Overview of the Control and Reserve Management Strategies", *IEEE Industrial Electronics Magazineno*. Vol. 7, No. 4. December 2013, pp. 42–55.

[5] J. M. Guerrero, J. C. Vasquez, J. Matas, L. G. De Vicuña, and M. Castilla, "Hierarchical control of droop-controlled AC and DC

microgrids - A general approach toward standardization", *IEEE Trans. Ind. Electron.*, vol. 58, no. 1, pp. 158–172, 2011.

[6] A. Bidram, S. Member, and A. Davoudi, "Hierarchical Structure of Microgrids Control System", pp. 1–14, 2012.

[7] J. A. P. Lopes, S. Member, C. L. Moreira, and A. G. Madureira, "Defining Control Strategies for Analysing MicroGrids Islanded Operation", pp. 1–7, 2002.

[8] Prabha Kundur, "*Power System Stability and Control*", McGraw-Hill, p. 1176, 1994.

[9] N. Pogaku, S. Member, M. Prodanovic, T. C. Green, and S. Member, "Modeling, Analysis and Testing of Autonomous Operation of an Inverter-Based Microgrid", *IEEE Transactions on power electronics*, vol. 22, no. 2, pp. 613–625, 2007.

[10] F. Katiraei, M. R. Iravani, and P. W. Lehn, "Small-signal dynamic model of a micro-grid including conventional and electronically interfaced distributed resources", *IET Gener. Transm. Distrib.*, vol. 1, no. (3), pp. 369–378, 2007

[11] J. M. Undrill, "Dynamic Stability Calculations for an Arbitrary Number of Interconnected", *IEEE Trans. Power Appar. Syst.*, no. 3, pp. 835–844.

[12] O. W. Paul C Krause Scott D. Sudhoff, *Analysis of Electric machinery and Drive Systems*. Wiley, 2002.

[13] S. Chung, "Phase-locked loop for grid-connected three-phase power conversion systems", *IEE Proc. - Electr. Power Appl.*, vol. 147, no. 3, pp. 213–219.

[14] A. Yazdani and R. Iravani, "A unified dynamic model and control for the voltage-sourced converter under unbalanced grid conditions", *IEEE Trans. Power Deliv.*, vol. 21, no. 3, pp. 1620–1629, 2006.

[15] IEEE, "Microgrid Stability Definitions, Analysis, and Modeling - Technical Report (PES-TR66)", *IEEE Power Energy Soc.*, no. April, p. 120, 2018.

[16] D. Baimel, J. Belikov, J. M. Guerrero, and Y. Levron, "Dynamic Modeling of Networks, Microgrids, and Renewable Sources in the dq0 Reference Frame: A Survey", *IEEE Access*, vol. 5, pp. 21323–21335, 2017.

APPENDIX

The state-space matrices of the power circuit and control system of VSI are described in (13), (21).

Power circuit of VSI from (12)

$$\dot{\Delta x}_{IXGin} = A_n \Delta x_{IXGin} + B_n^{vdq} \Delta v_{dqn} \tag{30}$$

Vector Δx_{IXin} and Δv_{IXGin} need to be expressed in the global rotating reference frame dq^g

$$\begin{aligned} \Delta x_{IXG} &= T_n^0 \Delta x_{IXGin} + i_\delta^0 \Delta\delta \\ \Delta v_{IXG} &= T_n^0 \Delta v_{IXGin} + v_\delta^0 \Delta\delta \end{aligned} \tag{31}$$

Where: $i_\delta^0 = [-i_q^{g0}, i_d^{g0}]^T$; $v_\delta^0 = [-v_q^{g0}, v_d^{g0}]^T$; $T_n^0 = \begin{bmatrix} \cos\delta_n^0 & -\sin\delta_n^0 \\ \sin\delta_n^0 & \cos\delta_n^0 \end{bmatrix}$

$$\begin{aligned} \Delta x_{IXGin} &= \left(T_n^0\right)^{-1} \Delta x_{IXG} - \left(T_n^0\right)^{-1} i_\delta^0 \Delta\delta \\ \Delta v_{IXGin} &= \left(T_n^0\right)^{-1} \Delta v_{IXG} - \left(T_n^0\right)^{-1} v_\delta^0 \Delta\delta \end{aligned} \tag{32}$$

The differential equation of (31)

$$\begin{aligned} \dot{\Delta x}_{IXG} &= \dot{T}_n^0 \Delta x_{IXGin} + i_\delta^0 \dot{\delta} = \dot{T}_n^0 \left(A_n \Delta x_{IXGin} + B_n^{vdq} \Delta v_{dq}\right) + i_\delta^0 \dot{\delta} \\ &= \dot{T}_n^0 A_n \left(T_n^0\right)^{-1} \Delta x_{IXG} - \dot{T}_n^0 A_n \left(T_n^0\right)^{-1} i_\delta^0 \Delta\delta + \dot{T}_n^0 B_n^{vdq} \Delta v_{dq} + i_\delta^0 \dot{\delta} \end{aligned} \tag{33}$$

In (33), $\Delta\delta$ can be deduced as a function of voltage angle $\Delta\theta$ in the local dq^n reference frame.

$$\Delta\delta = M_n \left(T_n^0\right)^{-1} \Delta v_{IXG} - \Delta\theta \tag{34}$$

$$M_n = \begin{bmatrix} \dfrac{-v_{DG,q}^0}{\left(v_{DG,q}^0\right)^2 + \left(v_{DG,d}^0\right)^2} & \dfrac{v_{DG,d}^0}{\left(v_{DG,q}^0\right)^2 + \left(v_{DG,d}^0\right)^2} \end{bmatrix} \tag{35}$$

The state-space equation in (13) is obtained by substituted for $\Delta\delta$ from (34) to (33):

$$\begin{aligned} \dot{\Delta x}_{IXG} = A_P \Delta x_{IXG} &+ B_P^{vIXG} \Delta v_{IXG} + B_P^{\theta} \Delta\theta + B_P^{\omega r} \Delta\omega_r \\ &+ B_P^{vdq} \Delta v_{dq} \end{aligned}$$

Where: $A_P = T_n^0 . A_n . \left(T_n^0\right)^{-1}$; $B_P^{vIXG} = B_n^{\delta n} . M_n . \left(T_n^0\right)^{-1}$

$B_n^{\delta n} = -T_n^0 . A_n . \left(T_n^0\right)^{-1} . i_\delta^0$; $B_P^{\theta} = T_{in}^0 . A_n . \left(T_n^0\right)^{-1} . i_\delta^0$ $B_P^{\omega r} = i_\delta^0 = [i_d^{g0}, -i_q^{g0}]^T$;

$B_P^{vdq} = T_n^0 . \begin{bmatrix} 1/L_f & 0 \\ 0 & 1/L_f \end{bmatrix}$

Control system of VSI from (14), (17), (19), (20)

$$\begin{aligned} \dot{\Delta x}_c = A_c \Delta x_c &+ B_c^{xIXGin} \Delta x_{IXGin} + B_c^{vIXGin} \Delta v_{IXGin} + B_c^{vdq} \Delta v_t \\ &+ B_c^{uIXG} \Delta u_{IXG} \end{aligned} \tag{36}$$

The state-space model in (21) is obtained through expressing Δx_{IXGn} and Δv_{IXGin} in the global rotating reference frame dq^g.

$$\begin{aligned} \dot{\Delta x}_c = A_c \Delta x_c &+ B_c^{xIXG} \Delta x_{IXG} + B_c^{vIXG} \Delta v_{IXG} + B_c^{vdq} \Delta v_t \\ &+ B_c^{uIXG} \Delta u_{IXG} + B_c^{\theta} \Delta\theta \end{aligned}$$

Where $B_c^{xIXG} = B_c^{xIXGin} \left(T_n^0\right)^{-1}$;

$$B_c^{xIXGin} = \begin{pmatrix} 0 & 0 & 0 & 0 & 1/T_i & 0 & 0 & 0 & 0 & 0 & 0 & 0 \\ 0 & 0 & 0 & 0 & 0 & 1/T_i & 0 & 0 & 0 & 0 & 0 & 0 \end{pmatrix}^T$$

$$\begin{aligned} B_c^{vIXG} = B_c^{vIXGin} \left(T_n^0\right)^{-1} &- B_c^{vIXGin} \left(T_n^0\right)^{-1} v_\delta^0 M_n \left(T_n^0\right)^{-1} \\ &- B_c^{xIXGin} \left(T_n^0\right)^{-1} i_\delta^0 M_n \left(T_n^0\right)^{-1} \end{aligned} ;$$

$$B_c^{vIXGin} = \begin{pmatrix} 1/T_v & 0 & 0 & 0 & 0 & 0 & 0 & 0 & 0 & 0 & 0 & 0 \\ 0 & 1/T_v & 0 & 0 & 0 & 0 & 0 & 0 & 0 & 0 & 0 & 0 \end{pmatrix}^T$$

$$B_c^{vdq} = \begin{pmatrix} 0 & 0 & 1/T_v & 0 & 0 & 0 & 0 & 0 & 0 & 0 & 0 & 0 \\ 0 & 0 & 0 & 1/T_v & 0 & 0 & 0 & 0 & 0 & 0 & 0 & 0 \end{pmatrix}^T ;$$

$$B_c^{\theta} = B_c^{xIXGin} \left(T_n^0\right)^{-1} i_\delta^0 + B_c^{vIXGin} \left(T_n^0\right)^{-1} v_\delta^0$$